From surface seismic data to elastic reservoir parameters using a full wavefield approach

Aayush Garg, D. J. Verschuur, Siddharth Sharma, Delft University of Technology The Netherlands*

a.garg-1@tudelft.nl

Keywords

Elastic parameters, impulse responses, redatuming, velocity estimation, localized FWI, joint migration inversion and proximity transformation.

Summary

Estimating deep subsurface reservoir properties from surface seismic data is a challenging task. This challenge becomes even larger when a target area is situated below a complex overburden. In this paper, we demonstrate a noval process called JMI-res, based on Joint Migration Inversion (JMI), to estimate the reservoir elastic parameters from the surface seismic elastic data for a complex subsurface scenario. In JMI-res, we first obtain the accurate local impulse responses at the target depth level and then we apply a localized inversion scheme on the estimated impulse responses to get the reservoir elastic parameters. Moreover, the velocity estimation is an integral part of JMI, thus, we do not require an accurate pre-estimated velocity model in JMI-res. We also show that the redatuming step of JMI-res provides much more reliable impulse responses, compared to standard redatuming based on time reversal of recorded data, because multiple scattering and transmission effects are fully accounted for.

Introduction

Estimating deep subsurface reservoir properties from surface seismic data for a target situated below a complex overburden is a challenging task. One familiar approach is to obtain the accurate local impulse response (virtual source-receiver response) at the target depth level via redatuming (Wapenaar et al., 1992; Schuster and Zhou, 2006) and apply a localized inversion scheme to get the reservoir elastic parameters.

In this paper, we demonstrate a noval process called 'JMI-res', based on Joint Migration Inversion (JMI) (Berkhout, 2014b; Staal, 2015), to estimate the reservoir elastic parameters from the surface seismic data for a complex subsurface. This paper is an extension to Garg and Verschuur, (2017a), where we limited ourselves to the estimation of redatumed full-wavefields (virtual source-receiver responses) at the target level. In this paper, we go one step further and also estimate the target-oriented reservoir elastic parameters using the redatumed impulse responses.

In JMI-res, we properly account for all complex propagation (transmission) and scattering effects (internal multiples) during the redatuming step. We will also reiterate this by comparing the estimated impulse responses with the ones estimated via standard redatuming approach (Beryhill, 1984), based on time reversal of recorded data. The full JMI-res process (Figure 1) to estimate the localized elastic parameters from the surface seismic data comprises of three main steps:

- In the first step, we estimate the one-way down- and upgoing wavefields (P^+/P^-) at the target depth below the overburden, via Joint Migration Inversion (JMI) along with the estimation of velocity model (Berkhout, 2014b; Staal, 2015; Garg and Verschuur, 2017a).

- Next, these redatumed wavefields (P^+/P^-) above the reservoir are transformed into local impulse responses ($\mathbf{X}$) with sources and receivers virtually being located at the top-reservoir level via so-called proximity transformation (Costa et al., 2015; Garg and Verschuur, 2016).

- Finally, these newly obtained local impulse responses are used for local, target-oriented full waveform inversion (FWI-res) (Gisolf et al., 2012).

Theory

Joint Migration Inversion

Joint Migration Inversion (JMI), as described by Berkhout (2012) and further developed by Berkhout

(2014b) and Staal (2015), is a data-driven, closed-loop inversion process that simultaneously optimizes the propagation velocity and the reflectivity associated with the subsurface while inherently estimating the down- and upgoing wavefields (P^+/P^-) at each subsurface depth level. It uses Full Wavefield Modeling (FWMod) (Berkhout, 2014a) as the forward modelling engine. FWMod explains the data in terms of propagation (**W**) and scattering (**R**)

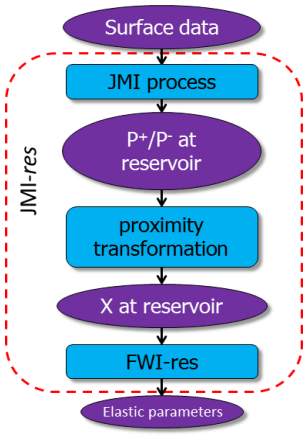

Figure 1: JMI-res flowchart.

operators, and most importantly, models all orders of scattering (primaries + internal multiples) and transmission effects. This correct handling of internal multiples is essential for accurate estimation wavefields estimation at target depth as shown by Garg and Verschuur (2016). The full JMI process can be understood by Figure 2. Moreover, in JMI, we do not explicitly impose a wave equation on the **W** and **R** operators. Therefore, These operators have the restricted freedom to vary in order to explain the input dataset. Thus, JMI has the ability to explain the elastic nature of the input data, especially regarding the amplitudes, without explicitly imposing the elastic wave equation (Garg and Verschuur, 2017b).

Proximity Transformation

The up- and downgoing wavefields at target depth level z_d, estimated by JMI, can be related as follows:

$$\vec{P}^-(z_d;z_0) = X(z_d,z_d)\vec{P}^+(z_d;z_0), \qquad (1)$$

where $\vec{P}^+(z_d;z_0)$ and $\vec{P}^-(z_d;z_0)$ represent the

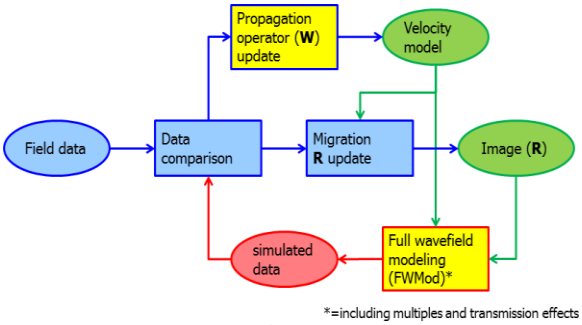

Figure 2: JMI implementation flowchart.

down- and upgoing wavefields at datum level z_d while X represents the impulse responses from the area below z_d. Note that these matrix symbols refer to multi-shot data in the space-frequency domain. The impulse responses at the target level are estimated via Proximity Transformation, which is a least-squares inversion process applied to equation 1 with sparsity and reciprocity constraints (Garg and Verschuur, 2016). The constrained objective function for this inversion process is given by:

$$J = \left(\frac{1}{\sigma_n^2}\right)\sum_w\sum\left\|\vec{P}^-(z_d,z_0) - \hat{X}(z_d,z_d)\vec{P}^+(z_d,z_0)\right\|_2^2$$
$$+\varepsilon_1^2\sum_\omega L_1[\hat{x}(z_d,z_d)] + \varepsilon_2^2\sum_\omega L_2[\hat{x}(z_d,z_d)]. \qquad (2)$$

The first term is the residual term. The second term is the sparsity constraint i.e., a L1-L2 norm that promotes sparsity in the time domain impulse responses function represented by $\hat{x}$. The third term is the reciprocity constraint to impose the principle of reciprocity (Knopoff and Gangi, 1959). The ε_i (i=1;2) and σ_n are different weights applied in the minimization process.

Target-oriented full waveform inversion (FWI-res)

FWI-res (Gisolf et al., 2012) is a non-linear, target-oriented inversion method in which the modelled reservoir responses are compared to the estimated reservoir impulse responses and the local elastic parameters are estimated. The implementation of this approach is done in the linear Radon domain with a locally laterally homogeneous medium assumption (i.e. local 1.5D assumption) at the target area. Hence, the input data, being the estimated local impulse

responses, is sorted in the common midpoint-offset domain (CMP) and transformed to the linear Radon domain before the inversion. The forward modeling engine used in FWI-res is the full elastic scattering integral (Fokkema and van den Berg, 1993). In FWI-res, we invert for κ, M and ρ properties which are linked to v_p and v_s as follows:

$$v_p = \sqrt{\frac{1}{\rho}\left(\frac{1}{\kappa} + \frac{4}{3M}\right)}, \quad v_s = \sqrt{\frac{1}{\rho M}}. \qquad (3)$$

Here, κ is the inverse of bulk modulus (K) and M is the inverse of shear modulus (μ). In FWI-res, the earth is parameterized as continuous property contrasts (χ) against a background. Thus, we actually solve for contrasts (χ) of elastic properties (equation 4) against the given background, instead of property contrasts across interfaces:

$$\chi_\kappa = \frac{\kappa - \kappa_b}{\kappa_b}, \quad \chi_M = \frac{M - M_b}{M_b}, \quad \chi_\rho = \frac{\rho - \rho_b}{\rho_b}. \qquad (4)$$

Numerical Example

We use a 2D subsurface model with three high velocity anomalies (v_p and v_s) and high densities (ρ) as overburden (Figure 3) to generate the input elastic data. In this example, our focus is only to explain the P-P reflection data and not the converted waves. Thus, to minimize the converted waves in the elastic input data, we have smoothed the overburden lenses boundaries in the S-wave velocity (v_s) and density (ρ) models.

The input data is generated via a finite difference implementation of the elastic wave equation (Thorbecke and Draganov, 2011). We use sources and receivers at 20m intervals and a Ricker wavelet of peak frequency 20 Hz as source, to generate the input elastic data. The topmost water layer ensures that we only record the P-mode elastic data at acquisition surface. Thus, the input data comprises of scalar pressure wavefields that are free of surface-related multiples (Figure 4a). To further decrease the converted waves at large offsets, we apply high-angle filtering to the input data in the linear Radon domain (Figure 4b). This filtered data (Figure 4b) acts as the processed input data in this example.

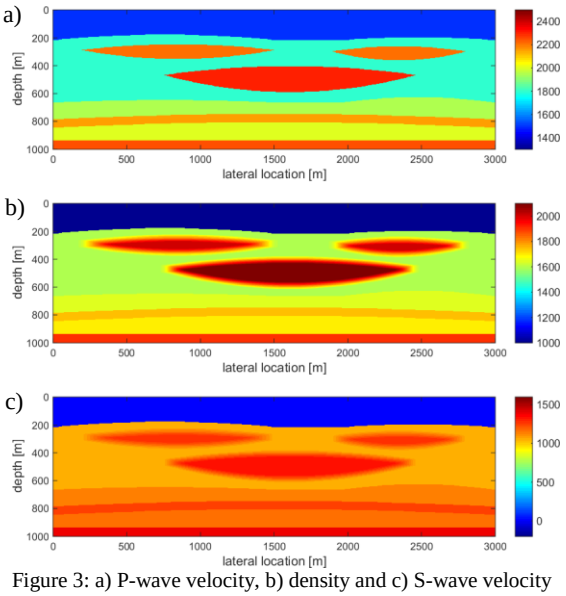

Figure 3: a) P-wave velocity, b) density and c) S-wave velocity models used to generate the elastic FD modelled input data.

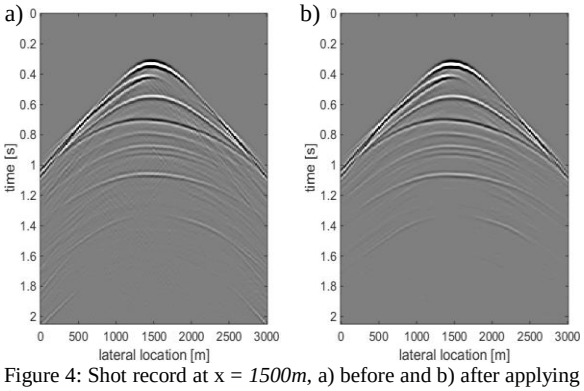

Figure 4: Shot record at x = *1500m*, a) before and b) after applying filtering at high plane-wave angles in the linear radon domain.

We apply JMI, i.e., the first step in the JMI-res strategy to estimate the down- and upgoing wavefields (P^+/P^-) at the target depth. The JMI step is applied as explained in Garg and Verschuur (2017a). Figure 5a,b shows the estimated velocity and structural image via JMI. We get a good estimate of the propagation velocity, which is further validated by the flat reflectivity angle gathers in Figure 6. Figure 7 shows the corresponding estimated down- and upgoing wavefields at the target depth of z_d =*680 m.* The limited offsets in the upgoing wavefields (P^-) (Figure 7b) are due to the limited receiver-aperture for the used acquisition geometry.

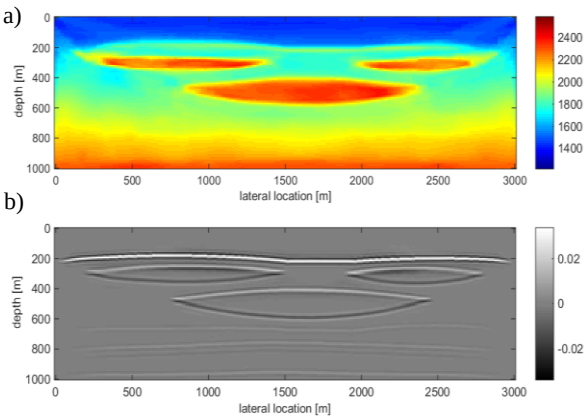

Figure 5: a) Estimated velocity model and b) estimated structural image via JMI.

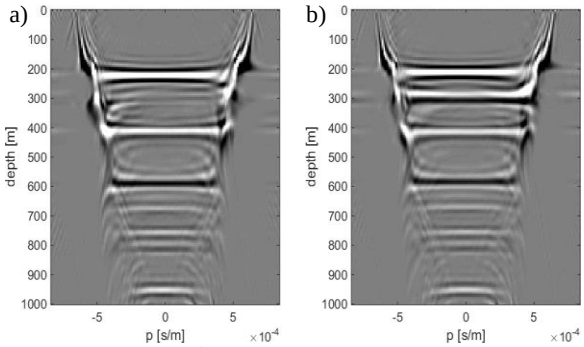

Figure 6: Estimated reflectivity angle-gathers at position a) $x = 1400m$ and b) $x = 1500m$ via JMI.

The down- and upgoing wavefields at target depth ($z_d = 680m$) are used to estimate the impulse responses i.e., the virtual source-receiver data, via proximity transformation which is the second step in the JMI res process. In Figure 8a, we can see the estimated impulse responses with three clear reflections corresponding to the target. As a comparison, we also estimated the impulse responses via a conventional standard redatuming, based on time reversal of recorded data. The impulse responses via standard redatuming (Figure 8b) are dominated by spurious events related to the internal multiples and converted waves in the overburden, even though we used a good velocity model estimated in the JMI step for standard redatuming. Thus, the impulse responses estimated in JMI-res are much more accurate than via standard redatuming. As a result, we will get much more accurate elastic parameters in the localised inversion step of JMI-res.

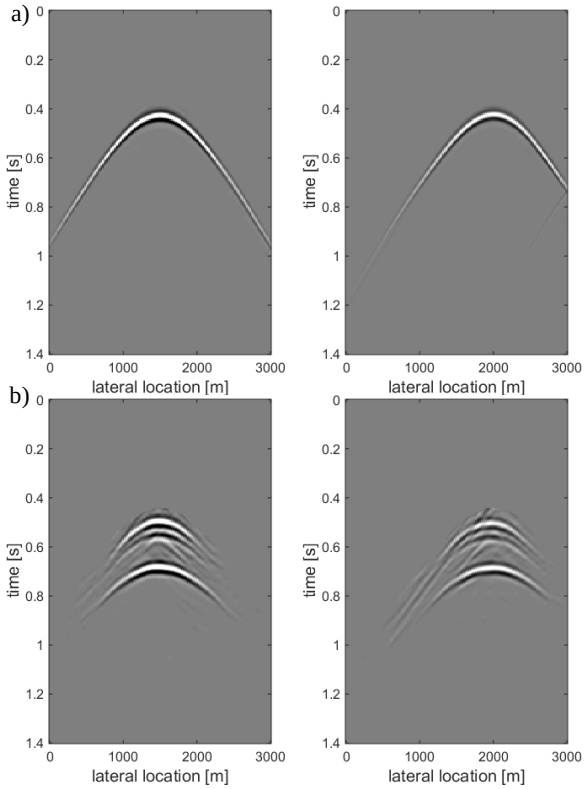

Figure 7: Estimated a) down- and b) upgoing wavefields for two lateral locations $x=1500m$ (left) and $x=2000m$ (right) at $z_d = 680m$ via the JMI process.

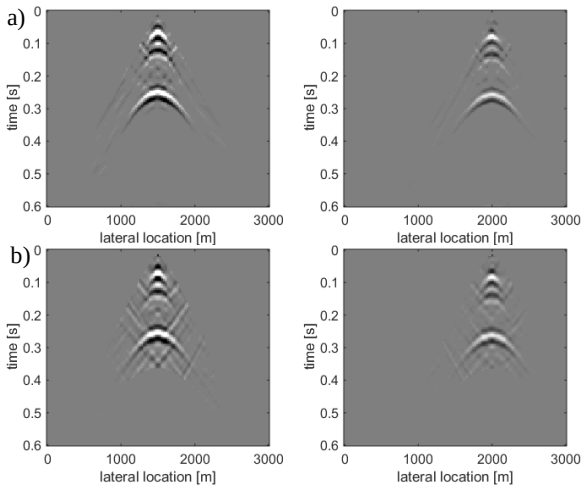

Figure 8: Estimated impulse responses for two lateral locations $x=1500m$ (left) and $x=2000m$ (right) at $z_d = 680m$ a) via the JMI-res process and b) via standard redatuming.

Before applying the last step i.e., FWI-res, in the JMI-res strategy to estimate the elastic parameters we transform the impulse responses in CMP-linear Radon domain. Moreover, we also require a wavelet estimate at the target depth to apply the localised inversion (FWI-res). We assume that we have a well log at the central location of the model (Figure 9a), which is usually the case in real field data. The wavelet (Figure 9b) at the target depth is estimated by least-squares matching of the estimated (in JMI-res) and modelled (via elastic scattering integral using well log information) impulse responses at the well location (Figure 9b). The local inversion domain for this example is depicted by the blue square box in

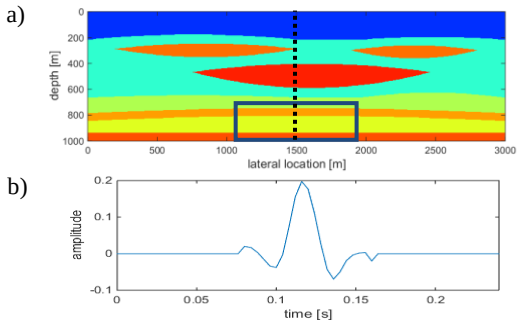

Figure 9: a) Diagram depicting the well location (dotted black line) at *x=1500m* and target domain (blue box) for the localised FWI-res. b) Estimated wavelet at the target depth level.

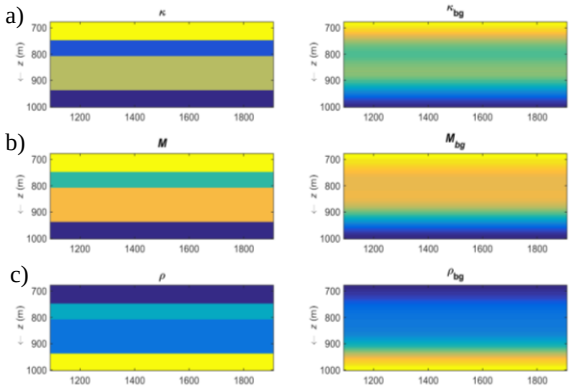

Figure 10: a) True and b) background κ (left), M (middle) and ρ (right) in the target domain.

Figure 9a. The inversion is done for the corresponding κ, M and ρ contrast functions (χ) (equation 4)**.** The background models for the elastic parameters (Figure 10b) are estimated from the background v_p, v_s and ρ using the relations in equation 3**.** Note, that the background v_p, v_s and ρ in the target area is taken identical to the one obtained at the well log location.

Figure 11a shows the estimated contrast functions (χ) via FWI-res for the central CMP location at *x=1500m*. We see a very good match between the estimated and true contrast functions. This match further improves after filtering the results to the temporal seismic bandwidth (Figure 11b). The mismatch in χ_ρ is due to the limited angles present in the impulse responses and requires further P-S data for more resolution. Figure 12 shows the estimated elastic parameters contrast functions for the whole target domain obtained after applying FWI-res at all the CMP locations. Again, we see a decent match between the estimated and true values. The incoherency and loss of resolution at some CMP locations depicts the kinematics uncertainty inherited due to the inaccuracies in the overburden velocity

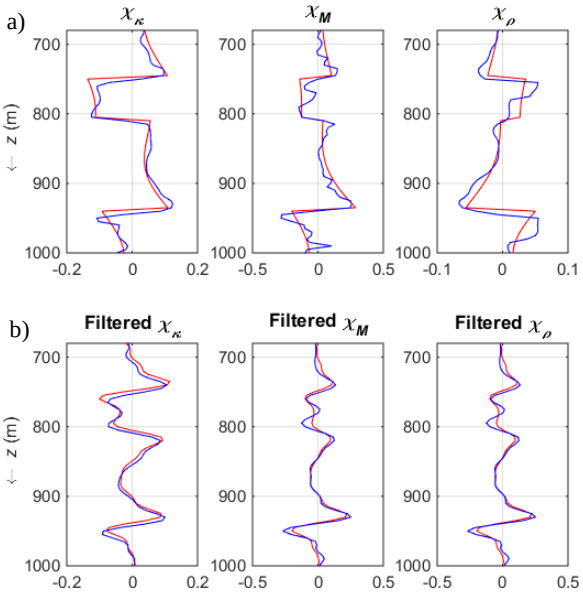

Figure 11: a) True (red) and Estimated (blue) contrast functions of κ (left), M (middle) and ρ (right) for central cmp location at *x=1500m* in the target domain. b) Corresponding contrast functions filtered to temporal seismic bandwidth.

estimation and requires some more prior information or knowledge of interpretation results such as marker horizons. In all, the JMI-res strategy has the promise of estimating the localised elastic parameters from

the surface data even in complex overburden scenarios.

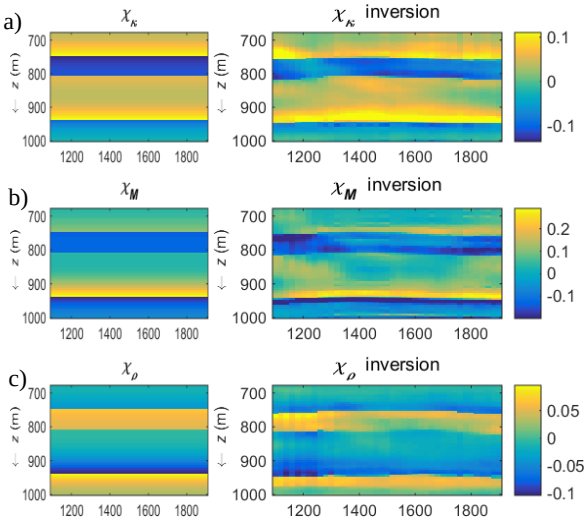

Figure 12: True (left) and Estimated (right) contrast functions of a) κ , b) M and c) ρ for the whole target domain.

Conclusions

In this paper, we convincingly demonstrated the ability of JMI-res to estimate the reservoir elastic parameters from the surface seismic elastic data for a complex subsurface scenario. We also showed that the local impulse responses estimated at the target depth level in JMI-res are much more accurate than what we get via standard redatuming. Another attractive feature of JMI-res which we showed is the inherent estimation of velocity model in the JMI-step. The natural next step in this research is to implement the whole JMI-res procedure on a field dataset. The future work will also involve incorporating converted waves in JMI-res, thus also explaining the P-S data, as proposed by Berkhout (2014a).

References

Berkhout, A. J., 2012, Combining full wavefield migration and full waveform inversion, a glance into the future of seismic imaging: Geophysics, 77, S43–S50.

Berkhout, A. J., 2014a, Review paper: An outlook on the future of seismic imaging, Part I: forward and reverse modelling: Geoph. Prosp., 62, no. 5, 911–930

Berkhout, A.J., 2014b, Review paper: An outlook on the future seismic imaging, Part III: Joint Migration Inversion. Geoph. Prosp., 62(5), 950–971.

Beryhill, J.R., 1984, Wave-equation datuming before stack. Geophysics, 49, 2064–2066.

Costa, A., Soni, A.K. and Verschuur, D.J., 2015, Using mutiples to improve the reservoir response via sparse inversion. SEG, Soc. Expl. Geophys., Expanded abstracts, 2978–2983.

Fokkema, J. T. ., and van den Berg, P. M., 1993, Seismic applications of acoustic reciprocity: Elsevier Science Publishers B.V.

Garg, A., and D. J. Verschuur, 2016, Reservoir impulse response estimation using joint migration inversion: 78th Ann. Internat. Mtg., EAGE, Expanded Abstracts, Eur. Ass. of Geosc. and Eng., Expanded abstracts, 4pp.

Garg, A., and D. J. Verschuur, 2017a, Reservoir impulse response estimation using joint migration inversion: 79th Ann. Internat. Mtg., EAGE, Expanded Abstracts, Eur. Ass. of Geosc. and Eng., Expanded abstracts, 4pp.

Garg, A., and D. J. Verschuur, 2017b, Elastic reflectivity preserving full wavefield inversion: 87th Ann. Internat. Mtg., Soc. Expl. Geophys., Expanded abstracts, 5p (Accepted).

Gisolf, A., Tetyukhina, D., and Luthi, S., 2012, Full elastic inversion of synthetic seismic data based on an outcrop model (book cliffs): 82nd Ann. Internat. Mtg., Soc. Expl. Geophys., Expanded abstracts, 5p.

Knopoff, L. and Gangi, A.F., 1959, Seismic reciprocity. Geophysics, 24, 681–691.

Schuster, G.T. and Zhou, M., 2006, A theoretical overview of model-based and correlation-based redatuming methods. Geophysics, 71, SI103–SI110.

Staal, X.R., 2015, Combined imaging and velocity estimation by Joint Migration Inversion. Ph.D. thesis, Delft University of Technology.

Thorbecke, J. W., and Draganov D., 2011, Finite-difference modeling experiments for seismic interferometry: Geophysics, 76, H1–H18.

Wapenaar, K., Cox, H.L.H. and Berkhout, A.J., 1992, Elastic redatuming of multicomponent seismic data. Geophysical Prospecting, 40, 465–482.

Acknowledgements

The authors thank the sponsors of the Delphi consortium for their support.